https://doi.org/10.5194/egusphere-2026-1677
Preprint. Discussion started: 4 May 2026

Chemical characteristics and environmental drivers of nitrogen-containing organic aerosol formation in coastal and inland urban atmospheres in Myanmar

Ning Zhang[1,2], Jialiang Feng[2], Simon Patrick O'Meara[3,4], Ziyi Liu[5], Yingge Ma[6,7], Xinlei Ge[8], Wenjing Li[9], Piero Chiacchiaretta[10,11], Piero Di Carlo[10,11], Junfeng Wang[1*], Eleonora Aruffo[11,12]

1. Jiangsu Key Laboratory of Atmospheric Environment Monitoring and Pollution Control (AEMPC), Collaborative Innovation Center of Atmospheric Environment and Equipment Technology (CIC-AEET), School of Environmental Science and Engineering, Nanjing University of Information Science and Technology, Nanjing 210044, China
2. School of Environmental and Chemical Engineering, Shanghai University, Shanghai 200444, China
3. Department for Earth and Environmental Sciences, University of Manchester, Manchester, M13 9PL, UK
4. National Centre for Atmospheric Science, University of Manchester, Manchester, M13 9PL, UK
5. Guangdong Provincial Key Laboratory of Atmospheric Environment and Pollution Control, College of Environment and Energy, South China University of Technology, Guangzhou Higher Education Mega Center, Guangzhou 510006, China
6. Shanghai Academy of Environmental Sciences, Shanghai 200233, China
7. State of Environmental Protection Key Laboratory of the Formation and Prevention of Urban Air Complex, Shanghai, 200233, China
8. School of Energy and Environment, Southeast University, Nanjing 211189, China
9. Meteorological Development and Planning Institute of China Meteorological Administration, Beijing, 100081, China
10. Department of Advanced Technologies in Medicine & Dentistry, University "G.d'Annunzio" of Chieti-Pescara, Chieti 66100, Italy
11. Center for Advanced Studies and Technology-CAST, Chieti 66100, Italy
12. Department of Science, University "G.d'Annunzio" of Chieti-Pescara, Chieti 66100, Italy

*Corresponding author: Wang, Junfeng (wangjunfeng@nuist.edu.cn)

Abstract:

Nitrogen-containing organic compounds (NOCs) are important light-absorbing constituents of atmospheric $PM_{2.5}$ and can substantially influence aerosol radiative forcing, air quality, and climate. Previous studies have mainly focused on the source apportionment and concentrations levels of NOCs, while the mechanisms governing their formation and particle-phase partitioning remain insufficiently constrained,

https://doi.org/10.5194/egusphere-2026-1677
Preprint. Discussion started: 4 May 2026

particularly in tropical regions. Here, we aim to elucidate regional differences in NOCs characteristics in Myanmar, with emphasis on how relative humidity (RH) and precursor species influence their formation pathways. We report the first molecular-level spatio-temporal characterization of NOCs in Myanmar, identifying 1064 organic compounds in ESI^- mode, with NOCs contributing 14-21% of molecular formulas and 13-35% of total mass. Organic nitrates (ONs) dominated CHON species across all sites, with higher abundances in Mandalay than in Yangon. Two ubiquitous nitrophenols, nitrocatechol ($C_6H_5NO_4$) and dimethyl nitrocatechol ($C_8H_9NO_4$), showed strong covariance but a distinct dependence of their particle-phase $C_8H_9NO_4/C_6H_5NO_4$ ratio on RH. CHemistry with Aerosol Microphysics in Python (PyCHAM) box model simulations reveal that increasing RH enhances aerosol water content, strengthening Raoult effect and preferentially suppressing condensation of the less soluble $C_8H_9NO_4$. Seasonal increases in summertime OH further promote $C_6H_5NO_4$ formation. These two processes explain the observed RH dependence and demonstrate that the $C_8H_9NO_4/C_6H_5NO_4$ ratio reflects both aerosol liquid water content and oxidative aging, while remaining sensitive to precursor supply. These findings provide new constraints on nitrophenol evolution in humid tropical environments and improve interpretation of NOC sources and aging processes, thereby supporting more accurate assessments of their regional and global radiative impacts.

Keywords: nitrogen-containing organic compounds; nitrophenolic compounds; relative humidity effects; gas-to-particle partitioning; aging

1.Introduction

Nitrogen-containing organic compounds (NOCs) are abundant and important constituents of atmospheric aerosols (Li et al., 2025), accounting from around 10% up to 60% of the total aerosol nitrogen under typical urban (Yu et al., 2025; Yu et al., 2021), and playing a significant role in the global nitrogen cycle (Ma et al., 2024). In addition, NOCs have been identified as important precursors of secondary organic aerosol (SOA),

https://doi.org/10.5194/egusphere-2026-1677
Preprint. Discussion started: 4 May 2026

thereby contributing to air pollution, and posing potential risks to human health (Smith et al., 2009; Abudumutailifu et al., 2024).

Over the past decade, research on NOCs has mainly focused on source apportionment and concentrations levels (Lin et al., 2010; Samy et al., 2013; Priestley et al., 2018), and Yu et al. (2024) reported that biomass burning and secondary formation are dominant NOCs sources. Observational studies conducted in urban, rural, marine and forested environments have demonstrated pronounced spatial variability in the molecular composition and relative abundances of aerosol NOCs (Samy and Hays, 2013; Jiang et al., 2022; Lin et al., 2012a; Xu et al., 2023; Zeng et al., 2020; Geng et al., 2009). Such variability is largely attributed to the diversity of emission sources and the heterogeneity of formation mechanisms of aerosol NOCs (Ma et al., 2024). Furthermore, subsequent oxidation or nitration of certain NOCs by ozone (O_3), hydroxyl radical (OH), and nitrogen oxides (NO_x) can exacerbate the health risks associated with organic aerosols (Bandowe and Meusel, 2017).

In recent years, increasing attention has been directed toward the formation mechanisms of NOCs, for example, Ma et al. (2024) elucidated how fresh and aged biomass fuels emit distinct classes of NOCs during combustion. Organic nitrates (ONs) and nitrophenols are two classes of NOCs that have attracted considerable research attention. Aerosol-phase ONs play an important role in the atmospheric fate of NO_x and O_3 production (Lelieveld et al., 2016), and several analytical techniques have been developed for their direct quantification in both the gas and particle phases. For instance, Aruffo et al. (2022) and Rollins et al. (2012) applied thermal dissociation laser-induced fluorescence (TD-LIF) to measure ONs in chamber experiments and field observations. Xu et al. (2017) estimated the mass concentration of organic nitrogen in Beijing using aerosol mass spectrometry (AMS), whereas Yu et al. (2019) quantified ON mass concentrations in PM_1 based on measurements from a high-resolution time-of-flight aerosol mass spectrometer (HR-ToF-AMS).

Nitrophenols are important components of brown carbon, formed through both primary emissions from combustion processes and secondary atmospheric chemistry (Desyaterik et al., 2013; Harrison et al., 2005). Time-of-flight mass spectrometer (ToF-

https://doi.org/10.5194/egusphere-2026-1677
Preprint. Discussion started: 4 May 2026

MS), High Performance Liquid Chromatography (HPLC), and Gas Chromatography-Mass Spectrometry (GC-MS) have been widely employed to detect nitrophenols in cloud water and aerosol samples, as well as to investigate their sources, concentrations and formation mechanisms (Desyaterik et al., 2013; Harrison et al., 2005). Yu et al. (2019) identified three biogenic volatile organic compounds (VOCs) (α-pinene, limonene, and camphene) and one anthropogenic VOC (styrene) as key precursors contributing to the formation of particulate ONs in urban site in China. Biomass burning not only acts an important primary source of nitrophenols but also provides critical precursors for their secondary formation (Harrison et al., 2005; Laskin et al., 2015). However, owing to the limited commercial availability of nitrophenol standards, most studies have been restricted to the quantitative analysis of only a limited number of nitrophenolic compounds (Cai et al., 2022; Cao et al., 2023).

In Southeast Asia, particularly in Myanmar，air pollution is relatively severe and biomass burning occurs frequently (Zhang et al., 2022; Nway et al., 2020). Existing studies in Myanmar have mainly focused on the mass concentrations, chemical composition, and source apportionment of atmospheric particulate matter (Zhang et al., 2022; Zhang et al., 2024b), whereas systematic investigations into the characteristics and formation pathways of atmospheric NOCs remain limited. This study aimed to characterize the spatial variability of NOCs in ambient $PM_{2.5}$ samples collected from Yangon and Mandalay, Myanmar, using ultra-high-performance liquid chromatography coupled with orbitrap mass spectrometry (UHPLC-Orbitrap MS). In addition, the formation-related processes of high-abundance nitrophenolic compounds were investigated, with particular emphasis on the influences of relative humidity (RH) and precursor availability on their secondary formation. Molecular-level identification of aerosol NOCs provides critical insights into their precursors, sources, and formation pathways, thereby enhancing our understanding of atmospheric NOCs drivers.

2.Materials and methods

https://doi.org/10.5194/egusphere-2026-1677
Preprint. Discussion started: 4 May 2026

2.1 Sample collection

$PM_{2.5}$ samples were collected at two major urban sites in Myanmar, Yangon and Mandalay (Fig. S1), during 2016 and 2017. In Yangon, sampling was conducted using a medium-volume $PM_{2.5}$ sampler (flow rate was 0.3 m^3 min^{-1}, Guangzhou Mingye Huanbao Technology Company, China) deployed on the rooftop of a six-story building (about 20 m above the ground) in Hlaing Township (16°51′30″N, 96°8′0″E), located in the northwestern urban area. In Mandalay, samples were collected on the rooftop of a three-story building situated in a mixed residential and commercial area of Chan-aye-thazan township (21°58′0″N, 96°5′0″E). Daily $PM_{2.5}$ samples were collected during both winter and summer periods, including winter campaigns from 4-22 December 2016 in Yangon and from 26 December 2016 to 16 January 2017 in Mandalay, as well as summer campaigns from 10-29 April 2017 in Yangon and from 20 March to 7 April 2017 in Mandalay. In total, 72 $PM_{2.5}$ samples were obtained. Detailed descriptions of the sampling procedures can be found in Zhang et al. (2022).

2.2. Instrumental analysis

2.2.1 Determination of water-soluble organic nitrogen

The mass concentration of water-soluble organic nitrogen (WSON) in atmospheric particulate matter was calculated as the difference between the concentration of water-soluble total nitrogen (WSTN) and that of water-soluble inorganic nitrogen (WSIN), i.e., WSON = WSTN − WSIN, where WSIN was calculated as WSIN = $[NO_3^-]/62 \times 14 + [NH_4^+]/18 \times 14$. Here, $[NO_3^-]$ and $[NH_4^+]$ denote the mass concentrations of nitrate and ammonium, respectively, measured by ion chromatography. The mass concentration of WSTN was determined using a UV–visible spectrophotometer (TU-1901, China).

2.2.2 GC-MS analysis of organic compounds

20 μL methyl-β-D-xylanopyranoside (MXP) was spiked onto the filters (30 cm^2) as an internal standard. The filters were subsequently subjected to ultrasonic extraction with 20 mL of dichloromethane/methanol (1:1 v/v) for 20 minutes at room temperature

https://doi.org/10.5194/egusphere-2026-1677
Preprint. Discussion started: 4 May 2026

for three times. The combined extracts were concentrated to approximately 2-3 mL using a rotary evaporator, followed by filtration and derivatization with 100 μL of N,O-bis-(trimethylsilyl)-trifluoroacetamide (BSTFA, with 1% trimethylchlorosilane as catalyst) and 20 μL of pyridine at 75 ℃ for 45 min. Prior to injection, hexamethylbenzene was added as an injection standard to evaluate the recovery of the target compounds, which ranged from 80% to 120%.

The extracts were analyzed using GC-MS (Agilent 5975 MSD coupled with Agilent 6890 GC) to determine levoglucosan mass concentrations. The GC oven was programmed to start at 60 ℃ for 2 min, ramped to 300 ℃ at 5 ℃ min^{-1}, and held isothermally at 300 ℃ for 10 min. Detailed descriptions of the GC-MS settings and analytical procedures are provided in previous publications (Feng et al., 2013; Zhong et al., 2021).

2.2.3 UHPLC-MS analysis of polar organic compounds

A 12 cm^2 section of each sampling filter was ultrasonically extracted with 3 mL of methanol and 30 μL of ethylene diamine tetraacetic acid (EDTA) for 30 minutes, with ice added to the water bath to prevent temperature increases and decomposition of organic compounds. After standing for 15 minutes, the extract was filtered through a 0.45 μm PTFE syringe filter. The residual filter was subsequently extracted twice (using 2 mL of methanol with 20 μL of EDTA and 1 mL of methanol with 10 μL of EDTA, respectively). All filtered extracts were combined and evaporated to near dryness under a slow stream of high-purity nitrogen, then redissolved in 100 μL of water and acetonitrile mixture (*V*:*V* = 1:1). The redissolved solution was centrifuged at >11,000 rpm for 20 minutes, and 5 μL of the supernatant was injected for analysis using UHPLC (Dionex 3000, Thermo Scientific, USA) - Orbitrap MS (Thermo Scientific, USA).

3-Nitrophenol (3-NP) was utilized to estimate the semi-quantitative concentrations of the detected compounds based on peak areas (unit: ng m^{-3}). Detailed information for the HPLC separation setup, UHPLC-Orbitrap MS data analysis and quantification procedures can be founded in Text S1 and Figs. S2-S3. The instrument was calibrated weekly to ensure that the mass resolution in negative mode (ESI^-) was below 2 ppm. Blank samples were processed and analyzed in the same way for deduction of

https://doi.org/10.5194/egusphere-2026-1677
Preprint. Discussion started: 4 May 2026

background effects.

2.3. Box modeling

Observation interpretation was augmented through application of the CHemistry with Aerosol Microphysics in Python (PyCHAM) box model (O'meara et al., 2021) version 5.6.0 (available at https://github.com/simonom/PyCHAM). The model used v3.3.1 of the Master Chemical Mechanism (Rickard, 2025) to solve gas-phase chemistry, including gas-phase inorganics and the following gas-phase VOCs: methane, propane, α-pinene, benzene, ethylbenzene, m,o,p-xylene (Bloss et al., 2005; Jenkin et al., 1997; Jenkin et al., 2003; Saunders et al., 2003). The model treats gas-particle partitioning dynamically. It was run in Eulerian mode. Assuming zero-dimensional representation of a 1*1*1 km box, and a 3 m s^{-1} horizontal wind vector, gave an air change rate of $3x10^{-3}$ s^{-1}. Observations of NO_x, O_3, RO_2 and HO_2 from urban Asian sites were used to set representative influx rates of NO_x and aliphatic parent VOCs (Aung et al., 2019; Tan et al., 2018; Nelson et al., 2021).

Since the gas-particle partitioning of aromatic oxidation products was investigated here, specifically $C_6H_5NO_4$ and $C_8H_9NO_4$, influx rates of their parent VOCs (benzene for $C_6H_5NO_4$ and ethylbenzene and o,m,p-xylene for $C_8H_9NO_4$) were particularly important for accurately identifying drivers of particle-phase aromatic oxidation products. For summer in Yangon, rates were set to give aromatic parent VOC concentrations consistent with observations from May 2017 in Yangon (Aung et al., 2019). However, Zhang et al. (2022) show that the prevailing source of air is maritime during Yangon summer and continental for Yangon winter and Mandalay winter and summer, resulting in substantially lower particle-phase organic carbon loading during Yangon summer. Furthermore, we know from Nelson et al. (2021) that benzene concentrations in southern Asian cities can reach 10 ppb, eight times more than the 1.2 ppb maximum reported for Yangon summer by Aung et al. (2019).

Additionally, Myanmar is a major biomass-burning region (Amnuaylojaroen and Parasin, 2023); therefore, continental air is more prone to influence from open fire burning (e.g. agricultural residues and tropical forest) than maritime air. Whilst both

https://doi.org/10.5194/egusphere-2026-1677
Preprint. Discussion started: 4 May 2026

$C_6H_5NO_4$ and $C_8H_9NO_4$ were well correlated with levoglucosan in both cities (Fig. S4), indicating a biomass burning source for both, the emission ratios of the precursors vary substantially between urban biomass burning, with ratios around 3:1 for $C_8H_9NO_4$: $C_6H_5NO_4$ precursors (Krugly et al., 2014), and tropical forest or agricultural residue burning, which have ratios of 1:3 and 1:2, respectively (Andreae, 2019). Therefore, for all locations and times, the same influx rates of $C_8H_9NO_4$ precursors was used (those constrained against observations for Yangon summer), however, the $C_6H_5NO_4$ precursor influx rate was set three times greater in Mandalay winter and summer than in Yangon summer and two times higher in Yangon winter than in Yangon summer, ratios consistent with the relative organic carbon loadings reported in Zhang et al. (2022).

For PyCHAM simulations, RH, temperature, and seed particle concentration were constrained against Zhang et al. (2022) The pure component saturation vapour pressures of $C_6H_5NO_4$ and $C_8H_9NO_4$ were constrained by the observations of Fredrickson et al. (2022) who report a c* for $C_6H_5NO_4$ of the order 10^1 μg m^{-3}. Using the Nannoolal et al. (2008) method for vapour pressure prediction from the UManSysProp toolkit (Topping et al., 2016), the vapour pressure of $C_8H_9NO_4$ compounds was estimated to be an order of magnitude lower than for $C_6H_5NO_4$, and was therefore set at 10^0 μg m^{-3}. For other organics the Nannoolal et al. (2008) method was used to estimate pure component vapour pressures. Particle-phase solubilities were set to be consistent with those reported for similar compounds (Lee et al., 2000), where the $C_6H_5NO_4$ molecule is close to ideal due to its polar hydroxyl and nitro functional groups, whereas the $C_8H_9NO_4$ molecules have two orders of magnitude greater activity coefficient due to their additional non-polar functional groups. Solubility was assumed to vary linearly with particle water mole fraction, consistent with Kholod et al. (2011) Consequently, for both $C_6H_5NO_4$ and $C_8H_9NO_4$ the activity coefficient was assumed to be unity at zero particle water mole fraction, whilst for $C_6H_5NO_4$ diluted by water, the activity coefficient was set to 10, and for $C_8H_9NO_4$ it was set to 3000. In our implementation, the activity coefficient does not directly increase the effective vapour pressure of $C_8H_9NO_4$, instead, it modulates non-ideality in the mixed organic-aqueous

https://doi.org/10.5194/egusphere-2026-1677
Preprint. Discussion started: 4 May 2026

phase. Because solubility increases strongly with aerosol water content, the net effect of increasing RH is an enhancement of particle-phase partitioning for both nitrophenols, with a stronger response for $C_8H_9NO_4$.

The HO_2 uptake coefficient to particles was set to 0.2 following Jacob. (2000) Gas-phase HONO influx rate was assumed to vary linearly with gas-phase water content, and tuned to give HONO values comparable to those observed in Delhi in 2017 by Pawar et al. (2024) with a maximum of $4.8*10^{-17}$ mol s^{-1} for $1.2*10^{-6}$ mol cm^{-3} of gas-phase water during Yangon summer.

Testing showed the model required around 9 hours of spin-up (starting from midday local time) before concentrations settled, and therefore results were taken over the 24 hours of simulation from 9-33 hours through the simulation. Unless otherwise stated, PyCHAM results are arithmetic means over these 24 hours. Natural light intensity was determined by setting the day of year and relevant latitude and longitude following the parameterisation of Hayman. (1997) All relevant PyCHAM input files, and the simulation outputs, are archived at https://github.com/simonom/PyCHAM/releases/tag/v5.7.8.

2.4. Data analysis

The Van Krevelen (VK) diagram is widely used to illustrate the evolutionary pathways of organic mixtures to infer the potential sources of organic aerosols by classifying known categories of natural and anthropogenic organic compounds (Xie et al., 2021; Bianco et al., 2018). Based on the H/C and O/C ratios, the VK diagram can be divided into seven regions corresponding to common classes of compounds identified in dissolved organic matter (Table 1): (A) lipids-like compounds, (B) aliphatic/peptides-like compounds, (C) carboxylic-rich alicyclic molecules (CRAMs-like structures), (D) carbohydrates-like compounds, (E) unsaturated hydrocarbons, (F) aromatic structures, and (G) highly oxygenated compounds (HOC).

Table 1 Stoichiometric ranges of VK classes (Bianco et al., 2018)

https://doi.org/10.5194/egusphere-2026-1677
Preprint. Discussion started: 4 May 2026

Rank	Class	H/C	O/C
A	Lipids-like	1.5<H/C≤2.0	0≤O/C≤0.3
B	Aliphatic/peptides-like	1.5<H/C≤2.2	0.3<O/C≤0.67
C	CRAMs-like structures	0.67<H/C≤1.5	0.1≤O/C<0.67
D	Carbohydrates-like	1.5<H/C≤2.5	0.67<O/C<1.0
E	Unsaturated hydrocarbons	0.67<H/C≤1.5	O/C<0.1
F	Aromatic structures	0.2≤H/C≤0.67	O/C<0.67
G	Highly Oxygenated Compounds (HOC)	0.6<H/C≤1.5	0.67≤O/C≤1.0

The aromaticity index (AI) is a parameter used to represent the density of C=C double bonds in organic molecules. Koch et al. (2006) proposed a modified formula for AI that excludes the potential contribution of heteroatoms to C=C bond density (Equation 2). AI $\geqslant$ 0.67 is generally considered indicative of condensed aromatic structures, whereas AI > 0.50 indicates the presence of aromatic structures. When the calculated AI value is less than zero, it is set to zero. The equation for calculating AI is given as follows (Koch and Dittmar, 2006):

$$AI = \frac{1 + C - \frac{1}{2}O - S - \frac{1}{2}(N + H)}{C - \frac{1}{2}O - N - S} \quad (2)$$

3. Results and discussion

3.1 Characteristics of molecules in ESI$^-$ modes

The identified organic compounds were classified into six categories based on molecular composition: CHO, CHON, CHONS, CHN, CHNS, and CHOS. CHONS- compounds represent species containing only C, H, O, N, and S in the ESI$^-$ mode, and the other categories are defined analogously. CHN and CHNS compounds were rarely detected in the ESI$^-$ mode.

The number of organic compounds identified in the ESI$^-$ mode ranged from 562 to 1,318, with an average of 1,064 molecular formulas. Among these, CHO species accounted for the largest proportion (46-67%), followed by CHOS (13-25%) and CHON (14-21%). These results are consistent with the findings of Sun et al. (2025), who reported that CHO-, CHOS-, and CHON- compounds dominate aerosol

https://doi.org/10.5194/egusphere-2026-1677
Preprint. Discussion started: 4 May 2026

298 constituents in most regions.

299 The total mass concentration of organic compounds detected in the ESI$^-$ mode was
300 279.7 ± 87.6 ng m^{-3}. Specifically, the mass concentrations of CHO-, CHON-, and
301 CHOS- compounds were 164.3 ± 39.0 ng m^{-3}, 62.3 ± 31.8 ng m^{-3}, and 43.8 ± 18.6 ng
302 m^{-3}, respectively (Table S1). Their corresponding contributions to the total
303 concentration ranged from 49-73% for CHO species, 13-35% for CHON species, and
304 8-22% for CHOS species. Although the number proportion of CHON compounds was
305 lower than that of CHOS species, their contribution to the total mass concentration was
306 comparatively higher, indicating that CHON compounds possess higher average
307 molecular abundances and play a non-negligible role in the overall organic aerosol mass.
308

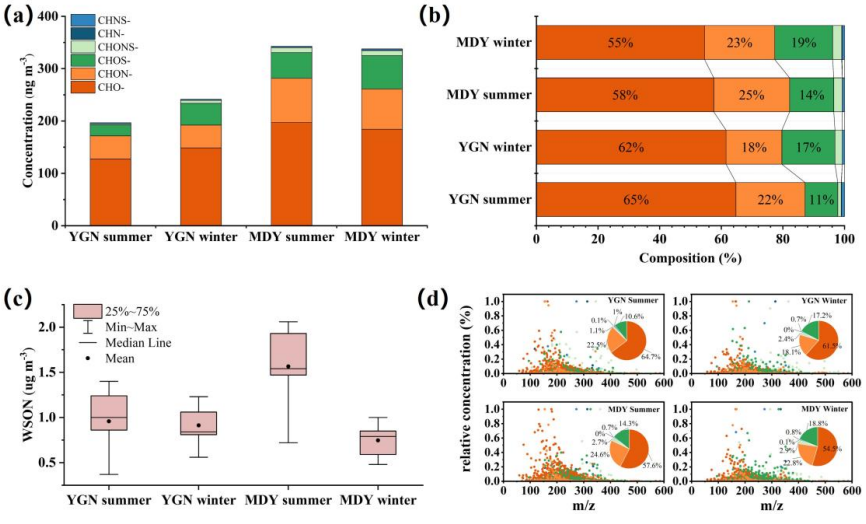

309
310 **Figure 1** Molecular characteristics of organic matter in Yangon (YGN) and Mandalay (MDY). **a**.
311 Semi-quantitative concentrations of CHO, CHON, CHOS, CHONS, CHN, and CHNS species
312 detected in both cities during summer and winter in the ESI$^-$ mode. **b**. Percentage contributions of
313 CHO, CHON, CHOS, CHONS, CHN, and CHNS species to the total molecular mass concentrations
314 in both cities during summer and winter in the ESI$^-$ mode. **c**. Mass concentration of WSON in both
315 cities during summer and winter. **d**. Reconstructed mass spectra of organic compounds derived from
316 extracted ion chromatograms in the ESI$^-$ mode. The vertical axis represents the semi-quantitative
317 normalized concentration of each compound. The pie charts illustrate the seasonal average
318 concentration contributions of different molecular species.
319

320 Significant differences in the mass concentrations and compositions of various

https://doi.org/10.5194/egusphere-2026-1677
Preprint. Discussion started: 4 May 2026

compound classes were observed between the two cities (Fig. 1a and Fig. 1b, Table S2). In the ESI^- mode, the mass concentrations of all compound types in $PM_{2.5}$ were higher in Mandalay than in Yangon during both winter and summer, consistent with the spatial distribution patterns of organic carbon (OC) (Zhang et al., 2024a).

The concentration proportion of CHO compounds was consistently higher in Yangon than in Mandalay (Yangon summer: 65%, Yangon winter: 62%, Mandalay summer: 58%, Mandalay winter: 55%). In contrast, CHON compounds accounted for a lower proportion in Yangon compared to Mandalay (Yangon summer: 22%, Yangon winter: 18%; Mandalay summer: 25%, Mandalay winter: 23%). The spatial distribution of CHOS concentration contributions exhibited a pattern similar to that of CHON, with higher fractions observed in Mandalay (Yangon summer: 11%, Yangon winter: 17%; Mandalay summer: 14%, Mandalay winter: 19%). Notably, the mass concentration of WSON, particularly during the MDY summer period, was substantially higher than those observed in the other three sampling periods (Fig. 1c). The results of the t-test showed that the WSON mass concentration in MDY summer was significantly different from that in YGN summer and MDY winter, with p values lower than 0.05 for both comparisons. These results indicate a statistically significant enhancement of WSON during the MDY summer period, and the underlying causes of the elevated WSON levels in MDY summer warrant further investigation. The reconstructed mass spectra of $PM_{2.5}$ samples collected in Yangon and Mandalay during winter, and summer are shown in Fig.1d. The molecular weights of the detected compounds were primarily distributed between 100 and 400, with majority of signal intensities concentrated between 100 and 200.

3.2 Spatial distribution characteristics of NOCs

3.2.1 Spatial distribution of organic nitrates

The formation of organic nitrates (ONs) enhances the partitioning of semi-volatile compounds into the particulate phase, thereby promoting SOA growth (Ng et al., 2007). Consequently, ONs are recognized as an important class of atmospheric compounds. In all Myanmar samples, 69-87% (mean: 77%) of CHON molecules met the structural

https://doi.org/10.5194/egusphere-2026-1677
Preprint. Discussion started: 4 May 2026

criterion of containing at least one -ONO_2 functional group (O/3N $\geqslant$ 1) and were preliminarily identified as ONs (Lin et al., 2012b; Wang et al., 2016). This result is consistent with the findings of Lin et al. (2012a), who reported that ONs constitute a major subclass of CHON- compounds in $PM_{2.5}$.

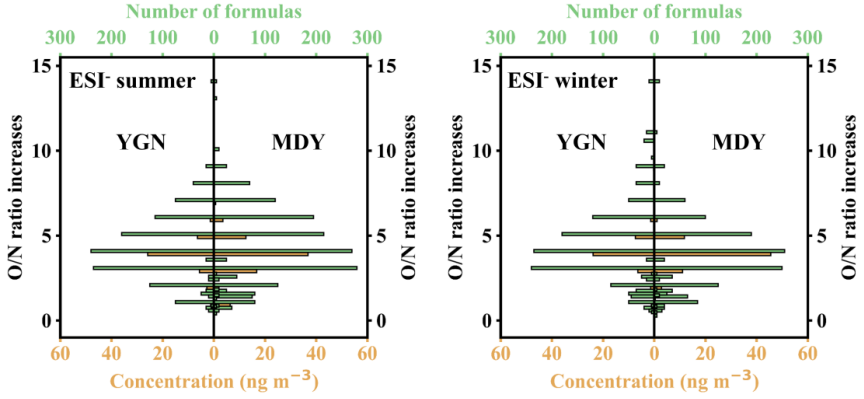

Figure 2 Classification of CHON compounds into subgroups based on O/N ratios in the ESI^- mode. Yellow and green colors indicate the ONs mass concentrations (ng m^{-3}) and number of species in each subgroup, respectively.

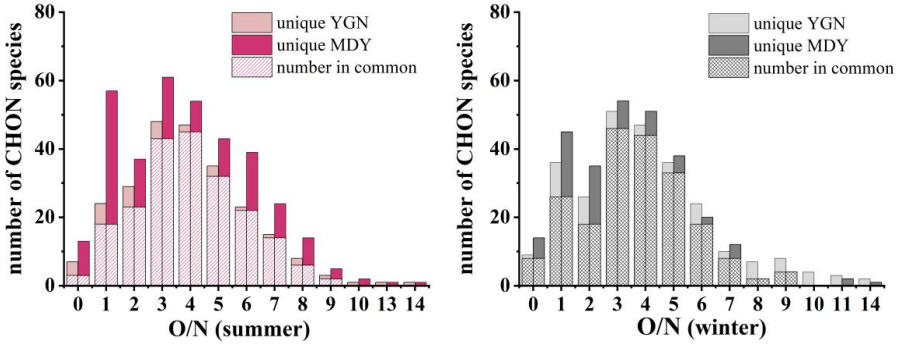

Figure 3 Numbers of common and region-specific compounds in MDY and YGN binned by O/N ratio. Number in common refers to the number of CHON compounds detected in both YGN and MDY, whereas unique YGN and unique MDY denote the numbers of CHON compounds detected exclusively in YGN and MDY, respectively.

As shown in Fig. 2, CHON compounds were classified into 32 subgroups according to their O/N ratios. A total of 245 CHON compounds were detected in the

https://doi.org/10.5194/egusphere-2026-1677
Preprint. Discussion started: 4 May 2026

Yangon summer samples, of which 75.1% were identified as ONs. 263 CHON compounds were detected in Yangon winter samples, with ONs accounting for 73.0% of the total CHON molecular species. Similarly, 351 and 278 CHON compounds were identified in the Mandalay summer and Mandalay winter samples, with ONs constituting 69.5% and 66.2%, respectively. The contributions of ONs to the total CHON compound mass concentrations in $PM_{2.5}$ were 89.5%, 91.5%, 84.4%, and 90.6% for Yangon summer, Yangon winter, Mandalay summer, and Mandalay winter, respectively. The remarkably high proportions of ONs in both molecular number and mass concentration indicate that ONs represent a dominant subgroup within CHON compounds.

In Fig. 2, pronounced differences in ON mass concentrations between the two sites are observed. The mass concentrations of ONs with O/N ratios higher than 3 in MDY were substantially higher than those in YGN (39.6 ng m^{-3}, 40.0 ng m^{-3}, 71.2 ng m^{-3}, and 69.7 ng m^{-3} for Yangon summer, Yangon winter, Mandalay summer, and Mandalay winter, respectively)，In contrast, the comparable overall mass contributions of ONs between the two sites were mainly attributable to the relatively higher mass concentrations of compounds with O/N < 3 in MDY than in YGN (4.7 ng m^{-3}, 3.7 ng m^{-3}, 13.1 ng m^{-3}, and 7.3 ng m^{-3} for Yangon summer, Yangon winter, Mandalay summer, and Mandalay winter, respectively). Further examination of CHON molecular formulas (Fig. 3) shows that, for most O/N ratio bins, the number of CHON compounds detected exclusively in MDY aerosols was higher than that detected exclusively in YGN aerosols, a pattern that was particularly pronounced in summer. These results indicate substantial differences in aerosol composition between the two cities, especially during MDY summer, exhibiting a more distinct molecular profile (Figs. 1c and 3).

3.2.2 Spatial distribution characteristics of nitrophenols

To more accurately identify types of NOCs, compounds containing aromatic rings were screened by combining AI values with the VK diagram. Molecular formulas that simultaneously met the criteria of O/N $\geqslant$ 3 and AI > 0.5 were classified as potential

https://doi.org/10.5194/egusphere-2026-1677
Preprint. Discussion started: 4 May 2026

nitrophenolic compounds. These compounds were primarily distributed across Zones C, F, and G of the VK diagram (Figs. 4 and 5). Bianco et al. (2018) reported that compounds with CRAMs-like structures (Zone C) may be associated with photochemical processing in aerosols, whereas HOC (Zone G) represent a group of extensively oxidized organics. Consequently, these two types of compounds are predominantly formed via secondary oxidation processes. Notably, mass concentration of these two compounds were higher in the Mandalay samples than in Yangon (Yangon summer: 40.2 ng m^{-3}, Yangon winter: 40.1 ng m^{-3}, Mandalay summer: 78.4 ng m^{-3}, Mandalay winter: 71.4 ng m^{-3}), suggesting that secondary formation processes play a more prominent role in $PM_{2.5}$ in Mandalay than in Yangon.

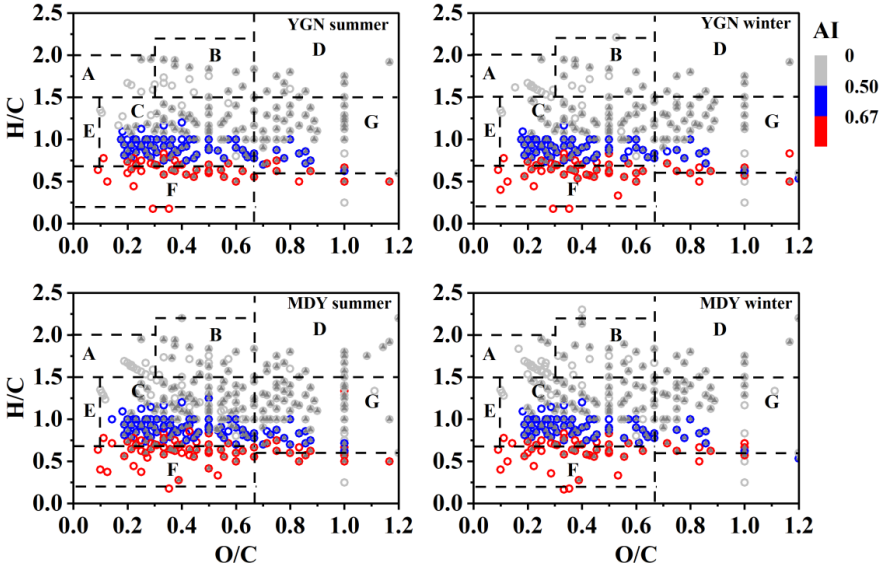

Figure 4 CHON- Van Krevelen (VK) diagram for the identified compounds. According to the H/C and O/C ratios, organic compounds are classified into seven categories (A-G). Color bars represent the aromaticity index (AI), while grey triangles denote compounds with O/N ⩾ 3.

The number of nitrophenolic compounds accounted for a relatively high proportion within Zone C (approximately 35%), with higher proportion observed in Yangon than in Mandalay during both seasons (Fig. 5). In Zone G, number of nitrophenolic compounds represented about 20% of all identified species. During summer, the number proportion of nitrophenolic compounds in Zone G was higher in

https://doi.org/10.5194/egusphere-2026-1677
Preprint. Discussion started: 4 May 2026

Yangon (22.9%) than in Mandalay (19.4%), whereas in winter, the trend was reversed, with Mandalay exhibiting a higher proportion (19.5%) compared to Yangon (16.3%).

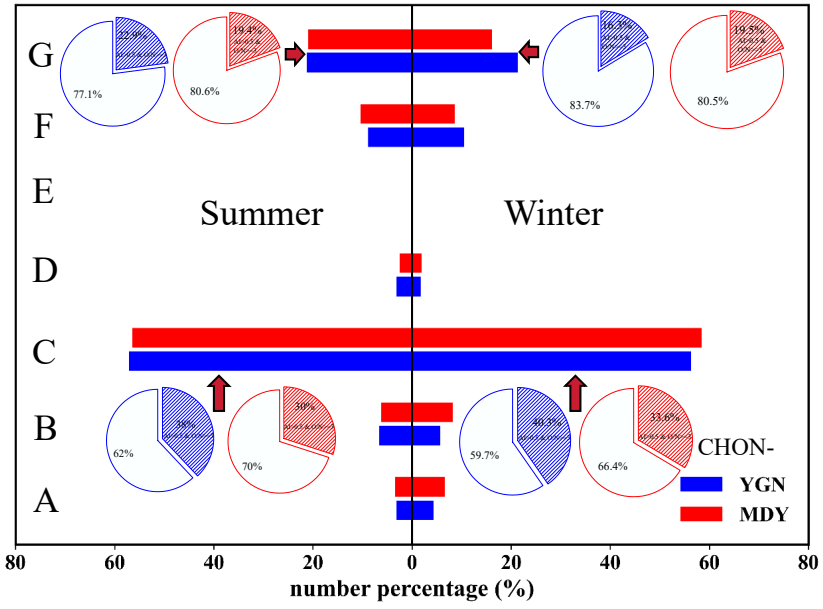

Figure 5 Percentage of CHON- subfraction groups (A-G). Shaded sections in the pie charts represent the number proportion of nitrophenolic compounds within each corresponding subgroup. Blue denotes the Yangon site, while red represents the Mandalay site.

3.3 $C_8H_9NO_4$ and $C_6H_5NO_4$

3.3.1 High detection efficiency NOCs

Compounds detected in all samples (detection frequency of 100%) were defined as common peaks. A total of 35 CHON compounds were identified as common peaks, and their reconstructed mass spectra were generated (Fig. S5). Among these, the two most abundant compounds corresponded to the molecular formulas $C_6H_5NO_4$ (m/z 154.01477) and $C_8H_9NO_4$ (m/z 182.04609), which were located in Zones G and C of Fig. 4, respectively. Based on literature reports, NIST library analysis, and the strong positive correlations of these compounds with levoglucosan (r = 0.76 and 0.73 for $C_8H_9NO_4$ and $C_6H_5NO_4$, respectively. Fig. S4), $C_6H_5NO_4$ and $C_8H_9NO_4$ were inferred to be nitrocatechol (Herich et al., 2011; Simoneit et al., 1991; Lin et al., 2018) and

https://doi.org/10.5194/egusphere-2026-1677
Preprint. Discussion started: 4 May 2026

dimethyl nitrocatechol (Claeys et al., 2012; Kourtchev et al., 2016), respectively.

Correlation analysis revealed a strong positive relationship between $C_6H_5NO_4$ and $C_8H_9NO_4$, suggesting that these two compounds share similar sources. However, under RH < 50%, the ratio of $C_8H_9NO_4/C_6H_5NO_4$ mass concentration changes with RH (Fig. 6). Samples collected during the Mandalay summer exhibited a relatively lower $C_8H_9NO_4/C_6H_5NO_4$ that coincided with a lower RH compared to the other sampling periods. According to our previous study (Zhang et al., 2022), the backward trajectories during both winter and summer in Mandalay were highly similar, indicating that the observed RH differences cannot be attributed to variations in air-mass transport. Collectively, these findings indicate that the formation of $C_6H_5NO_4$ and $C_8H_9NO_4$ is strongly associated with RH. The PyCHAM box model is applied to further investigate the factors influencing the formation of these two compounds.

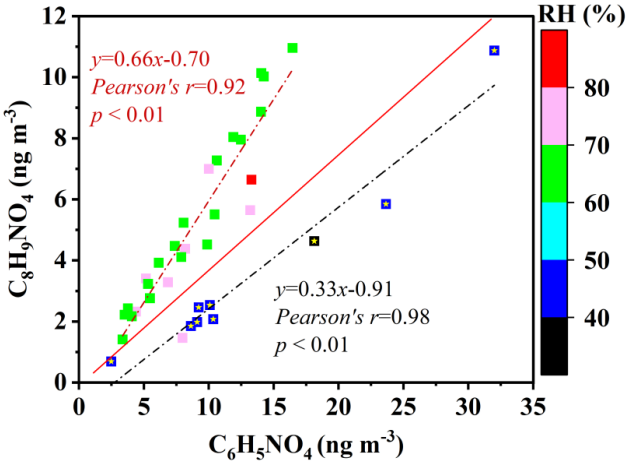

Figure 6 The correlation between $C_6H_5NO_4$ and $C_8H_9NO_4$. Color bar is relative humidity. Yellow stars represent MDY summer samples.

3.3.2 RH effect on $C_8H_9NO_4/C_6H_5NO_4$

Following application of the constraints to box modelling described in Section 2.3, six simulations were conducted to investigate the drivers of varying particle-phase $C_8H_9NO_4/C_6H_5NO_4$ ratio, three for Yangon and three for Mandalay. In Mandalay, the RH changed substantially between seasons, whilst simulated influx rates of precursors remained constant, whilst in Yangon, the RH was relatively consistent but simulated

https://doi.org/10.5194/egusphere-2026-1677
Preprint. Discussion started: 4 May 2026

459 influx rates of precursors changed with season. To help probe the effect of varying
460 photochemistry between seasons, one of the Yangon simulations is a hypothetical
461 scenario where the photochemistry was set to winter but the precursor influx was set to
462 summer conditions (Fig. S6).

463 The resulting simulations of particle-phase $C_8H_9NO_4$ and $C_6H_5NO_4$ reproduce
464 the observed trend of increasing $C_8H_9NO_4/C_6H_5NO_4$ ratio with increasing RH (Fig. 7).
465 Several factors are at play in the simulated results of Fig. 7: the increase in gas-phase
466 OH concentration from winter to summer (photochemistry effect), the increasing influx
467 rate of benzene from a minimum in Yangon summer to a moderate value in Yangon
468 winter and a maximum for both seasons for Mandalay, and the increasing pressure for
469 $C_8H_9NO_4$ and $C_6H_5NO_4$ to condense to the particle phase due to their decreased
470 particle-phase mole fraction resulting from increased aerosol water mole fraction under
471 increased RH (Raoult effect).

472 The effect of HO_2 uptake to particles and of HONO influx rate dependence on
473 gas-phase water content was tested by turning off HO_2 uptake and by setting HONO
474 influx rate to constant across simulations. Neither process showed a significant change
475 to the trend of increasing $C_8H_9NO_4/C_6H_5NO_4$ ratio with increasing RH.

476 Considering first just the Mandalay results, for which the influx rates of $C_6H_5NO_4$
477 and $C_8H_9NO_4$ precursors were constant across all RH, the decrease in gas-phase water
478 content from 80 to 60 % RH leads to a slight decrease in OH concentration, but the
479 change in consumption of the parent VOCs is negligible. Therefore, the cause for the
480 decrease in particle-phase $C_8H_9NO_4$ and $C_6H_5NO_4$ is the decreased Raoult effect arising
481 from decreased mole fraction of particle-phase water. The decrease in particle-phase
482 concentration of $C_8H_9NO_4$ from 80 to 60 % RH is 30 %, whilst the decrease is 10 % for
483 $C_6H_5NO_4$, with the greater sensitivity of $C_8H_9NO_4$ leading to the decrease in
484 $C_8H_9NO_4/C_6H_5NO_4$.

485 Whilst the Raoult effect continues to act to decrease condensation of $C_8H_9NO_4$ and
486 $C_6H_5NO_4$ as RH decreases from 60 % in Mandalay winter to 40 % in Mandalay summer,
487 the particle-phase loading of both $C_8H_9NO_4$ and $C_6H_5NO_4$ actually increases, driven by
488 the increased OH concentration that results from enhanced photochemistry. $C_6H_5NO_4$

https://doi.org/10.5194/egusphere-2026-1677
Preprint. Discussion started: 4 May 2026

appears to be particularly sensitive to changing atmospheric oxidising capacity, as its relative increase is greater than that of $C_8H_9NO_4$.

The Yangon results are all for 70 % RH, and therefore have similar Raoult effect. For the non-hypothetical Yangon results, a higher influx rate of $C_6H_5NO_4$ precursor in winter acts to decrease $C_8H_9NO_4/C_6H_5NO_4$ (Fig. S6). However, the hypothetical result for Yangon winter had the same influx rates of precursors as the Yangon summer simulation, and shows that the decrease in photochemistry from Yangon summer to Yangon winter acts to increase $C_8H_9NO_4/C_6H_5NO_4$, giving a result of approximately 1 (Fig. 7). Despite the substantial influence of photochemistry, the $C_8H_9NO_4/C_6H_5NO_4$ for Yangon winter with more realistic $C_6H_5NO_4$ precursor influx is below that of Yangon summer, showing that the effect of reasonable changes in precursor concentration can exceed the photochemistry effect.

The box modelling results have shown that the Raoult effect driven by changes in aerosol water content, which are driven by changes in RH, exerts a physical influence over $C_8H_9NO_4/C_6H_5NO_4$, since $C_8H_9NO_4$ is more sensitive to the effect. However, atmospheric oxidising capacity has also been identified as playing an influential role in explaining the observed changes in $C_8H_9NO_4/C_6H_5NO_4$. The box modelling results are consistent with observed changes in the BeP/(BeP+BaP) ratio ((where BeP (Benzo[e]pyrene) and BaP (Benzo[a]pyrene) data were taken from our previous study (Zhang et al., 2024b, Fig. S7). The BeP/(BeP+BaP) ratio has been widely used as an indicator of aerosol aging (Křůmal et al., 2013). Fig. S7 shows the highest BeP/(BeP+BaP) ratios for Mandalay summer and Yangon summer, supporting the box model result that photochemistry varies substantially between seasons. Because of the difference in sensitivity to changing oxidising capacity between $C_8H_9NO_4$ and $C_6H_5NO_4$, when all else is constant, the $C_8H_9NO_4/C_6H_5NO_4$ acts as an indicator of aerosol aging. However, the spread of points in Fig. S7, particularly for Yangon summer and Mandalay summer, combined with the box model findings above, demonstrate that varying precursor concentrations can substantially disrupt the relationship between $C_8H_9NO_4/C_6H_5NO_4$ and aerosol aging.

Considering the modelling and observation results discussed in this section, two

https://doi.org/10.5194/egusphere-2026-1677
Preprint. Discussion started: 4 May 2026

factors are suggested to contribute to the significantly greater WSON in Mandalay summer in Fig. 1. First, the high degree of oxidation of organics due to enhanced photochemistry relative to the winter scenarios. Second, the high concentration of precursors for relatively soluble oxidation products relative to Yangon summer (see Section 2.3 for discussion of why $C_6H_5NO_4$ is expected to be more water soluble than $C_8H_9NO_4$). However, a more thorough investigation involving more NOCs would be needed to test this hypothesis.

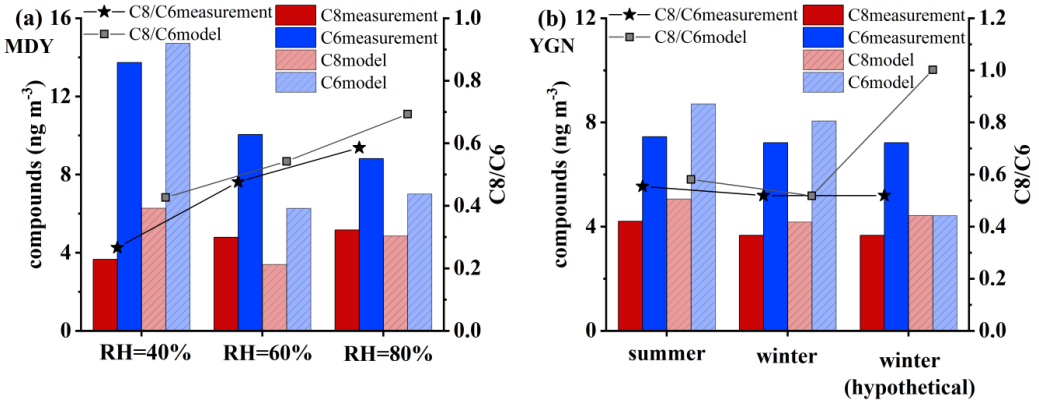

Figure 7 (a) Concentration distributions of $C_8H_9NO_4$ and $C_6H_5NO_4$ under different RH conditions in Mandalay. (b) Concentration distributions of $C_8H_9NO_4$ and $C_6H_5NO_4$ during Yangon summer, winter and winter hypothetical. Dark-colored bars represent the observed mass concentrations, while light-colored bars indicate the mass concentrations simulated by the model.

4. Atmospheric implications

This study provides new insights into the molecular characteristics and formation controls of NOCs in urban aerosols influenced by biomass burning. The results demonstrate that ONs and nitrophenolic compounds constitute major components of NOCs. By combining molecular-level observations with aromatic emission rates from combustion of varying biomasses and box model simulations, we show that variations in the formation of nitrophenolic compounds is influenced by changing RH, variations in precursor concentrations, and seasonal changes to photochemistry.

In particular, the effect of open burning of biomass combined with enhanced

https://doi.org/10.5194/egusphere-2026-1677
Preprint. Discussion started: 4 May 2026

photolysis acts to enhance $C_6H_5NO_4$ formation through increased benzene emission and OH concentration, respectively. This box model finding is supported by the higher concentrations of highly oxygenated compounds in the inland city of Mandalay, compared to coastal megacity of Yangon, underscoring the enhanced importance of open biomass burning in inland atmospheres. These results are consistent with previous studies identifying biomass burning as an important source of aromatic precursors and nitrophenolic compounds (Salvador et al., 2021; Wang et al., 2020). While further demonstrating how RH and photochemical conditions jointly regulate molecular-level partitioning and transformation of nitrophenolic compounds in tropical urban atmospheres.

In contrast, $C_8H_9NO_4$ formation rate is less affected by open biomass burning and photochemistry variation, but its gas-particle partitioning was shown to be relatively sensitive to changing RH, via the Raoult effect. These indicates that importance of accurate emission, photochemistry and gas-particle partitioning thermodynamics in predicting particle-phase composition and abundance in chemical transport models. However, due to the limited availability of standards, quantitative analysis was only possible for few nitrophenolic compounds. Future work should include more comprehensive laboratory simulations to better constrain the effects of RH and OH on the formation and degradation of nitrophenolic compounds.

Data availability. The data are available upon request from the corresponding author Junfeng Wang (wangjunfeng@nuist.edu.cn).

Author contributions. JF and YM designed the research. NZ conducted the measurements. NZ, JF, SO, ZL, JW and EA analysed the data. NZ, JF, SO, YM, XG, WL, PC, PDC, JW and EA reviewed and commented on the paper. NZ and SO wrote the paper.

Competing interests. The contact author has declared that none of the authors has any competing interests.

Financial support. This work was supported by the Natural Science Foundation of Jiangsu Province (No. BK20240036), National Natural Science Foundation of China (NOs. 22276099, U24A20515, 41877373, 42405113), Jiangsu Funding Program for Excellent Postdoctoral Talent (No. 2023ZB396), and the Guangxi Key Research and Development Program, China (No. Guike

https://doi.org/10.5194/egusphere-2026-1677
Preprint. Discussion started: 4 May 2026

AB24010074), the UK National Centre for Atmospheric Science.

Reference:

Abudumutailifu, M., Shang, X., Wang, L., Zhang, M., Kang, H., Chen, Y., Li, L., Ju, R., Li, B., Ouyang, H., Tang, X., Li, C., Wang, L., Wang, X., George, C., Rudich, Y., Zhang, R., and Chen, J.: Unveiling the molecular characteristics, origins, and formation mechanism of reduced nitrogen organic compounds in the urban atmosphere of Shanghai using a versatile aerosol concentration enrichment system, Environ. Sci. Technol., 58, 7099-7112, https://doi.org/10.1021/acs.est.3c04071, 2024.

Amnuaylojaroen, T. and Parasin, N.: Perspective on particulate matter: from biomass burning to the health crisis in mainland Southeast Asia, Toxics, 11, 553, 2023.

Andreae, M. O.: Emission of trace gases and aerosols from biomass burning – an updated assessment, Atmos. Chem. Phys., 19, 8523-8546, https://doi.org/10.5194/acp-19-8523-2019, 2019.

Aruffo, E., Wang, J., Ye, J., Ohno, P., Qin, Y., Stewart, M., McKinney, K., Di Carlo, P., and Martin, S. T.: Partitioning of organonitrates in the production of secondary organic aerosols from α-pinene photo-oxidation, Environ. Sci. Technol., 56, 5421-5429, https://doi.org/10.1021/acs.est.1c08380, 2022.

Aung, W.-Y., Noguchi, M., Pan-Nu Yi, E.-E., Thant, Z., Uchiyama, S., Win-Shwe, T.-T., Kunugita, N., and Mar, O.: Preliminary assessment of outdoor and indoor air quality in Yangon city, Myanmar, Atmos. Pollut. Res., 10, 722-730, https://doi.org/10.1016/j.apr.2018.11.011, 2019.

Bandowe, B. A. M. and Meusel, H.: Nitrated polycyclic aromatic hydrocarbons (nitro-PAHs) in the environment – a review, Sci. Total Environ., 581-582, 237-257, https://doi.org/10.1016/j.scitotenv.2016.12.115, 2017.

Bianco, A., Deguillaume, L., Vaïtilingom, M., Nicol, E., Baray, J.-L., Chaumerliac, N., and Bridoux, M.: Molecular characterization of cloud water samples collected at the puy de Dôme (France) by fourier transform ion cyclotron resonance mass spectrometry, Environ. Sci. Technol., 52, 10275–10285, https://doi.org/10.1021/acs.est.8b01964, 2018.

Bloss, C., Wagner, V., Jenkin, M. E., Volkamer, R., Bloss, W. J., Lee, J. D., Heard, D. E., Wirtz, K., Martin-Reviejo, M., Rea, G., Wenger, J. C., and Pilling, M. J.: Development of a detailed chemical mechanism (MCMv3.1) for the atmospheric oxidation of aromatic hydrocarbons, Atmos. Chem. Phys., 5, 641-664, https://doi.org/10.5194/acp-5-641-2005, 2005.

Cai, D., Wang, X., George, C., Cheng, T., Herrmann, H., Li, X., and Chen, J.: Formation of secondary nitroaromatic compounds in polluted urban environments, J. Geophys. Res-Atmos., 127, e2021JD036167, https://doi.org/10.1029/2021JD036167, 2022.

Cao, M., Yu, W., Chen, M., and Chen, M.: Characterization of nitrated aromatic compounds in fine particles from Nanjing, China: optical properties, source allocation, and secondary processes, Environ. Pollut., 316, 120650, https://doi.org/10.1016/j.envpol.2022.120650, 2023.

Claeys, M., Vermeylen, R., Yasmeen, F., Gómez-González, Y., Chi, X., Maenhaut, W., Mészáros, T., and Salma, I.: Chemical characterisation of humic-like substances from urban, rural and tropical biomass burning environments using liquid chromatography with UV/vis photodiode array detection and electrospray ionisation mass spectrometry, Environ. Chem., 9, 273-284, https://doi.org/10.1071/EN11163, 2012.

Desyaterik, Y., Sun, Y., Shen, X., Lee, T., Wang, X., Wang, T., and Collett Jr, J. L.: Speciation of "brown" carbon in cloud water impacted by agricultural biomass burning in eastern China, J. Geophys. Res-Atmos., 118, 7389-7399, https://doi.org/10.1002/jgrd.50561, 2013.

https://doi.org/10.5194/egusphere-2026-1677
Preprint. Discussion started: 4 May 2026

Feng, J., Li, M., Zhang, P., Gong, S., Zhong, M., Wu, M., Zheng, M., Chen, C., Wang, H., and Lou, S.: Investigation of the sources and seasonal variations of secondary organic aerosols in $PM_{2.5}$ in Shanghai with organic tracers, Atmos. Environ., 79, 614-622, https://doi.org/10.1016/j.atmosenv.2013.07.022, 2013.

Fredrickson, C. D., Palm, B. B., Lee, B. H., Zhang, X., Orlando, J. J., Tyndall, G. S., Garofalo, L. A., Pothier, M. A., Farmer, D. K., Decker, Z. C. J., Robinson, M. A., Brown, S. S., Murphy, S. M., Shen, Y., Sullivan, A. P., Schobesberger, S., and Thornton, J. A.: Formation and evolution of catechol-derived SOA mass, composition, volatility, and light absorption, ACS Earth Space Chem., 6, 1067-1079, https://doi.org/10.1021/acsearthspacechem.2c00007, 2022.

Geng, H., Park, Y., Hwang, H., Kang, S., and Ro, C. U.: Elevated nitrogen-containing particles observed in Asian dust aerosol samples collected at the marine boundary layer of the Bohai Sea and the Yellow Sea, Atmos. Chem. Phys., 9, 6933-6947, https://doi.org/10.5194/acp-9-6933-2009, 2009.

Harrison, M. A. J., Barra, S., Borghesi, D., Vione, D., Arsene, C., and Iulian Olariu, R.: Nitrated phenols in the atmosphere: a review, Atmos. Environ., 39, 231-248, https://doi.org/10.1016/j.atmosenv.2004.09.044, 2005.

Hayman, G.: Effects of pollution control on UV exposure, in: AEA technology final report. Reference AEA/RCEC/22522001/R/002 ISSUE1, Department of Health on Contract 121/6377, AEA Technology, Oxfordshire, UK., 1997.

Herich, H., Hueglin, C., and Buchmann, B.: A 2.5 year's source apportionment study of black carbon from wood burning and fossil fuel combustion at urban and rural sites in Switzerland, Atmos. Meas. Tech., 4, 1409-1420, https://doi.org/10.5194/amt-4-1409-2011, 2011.

Jacob, D. J.: Heterogeneous chemistry and tropospheric ozone, Atmos. Environ., 34, 2131-2159, https://doi.org/10.1016/S1352-2310(99)00462-8, 2000.

Jenkin, M. E., Saunders, S. M., and Pilling, M. J.: The tropospheric degradation of volatile organic compounds: a protocol for mechanism development, Atmos. Environ., 31, 81-104, https://doi.org/10.1016/S1352-2310(96)00105-7, 1997.

Jenkin, M. E., Saunders, S. M., Wagner, V., and Pilling, M. J.: Protocol for the development of the Master Chemical Mechanism, MCM v3 (Part B): tropospheric degradation of aromatic volatile organic compounds, Atmos. Chem. Phys., 3, 181-193, https://doi.org/10.5194/acp-3-181-2003, 2003.

Jiang, H., Li, J., Tang, J., Zhao, S., Chen, Y., Tian, C., Zhang, X., Jiang, B., Liao, Y., and Zhang, G.: Factors influencing the molecular compositions and distributions of atmospheric nitrogen-containing compounds, J. Geophys. Res-Atmos., 127, e2021JD036284, https://doi.org/10.1029/2021JD036284, 2022.

Kholod, Y. A., Gryn'ova, G., Gorb, L., Hill, F. C., and Leszczynski, J.: Evaluation of the dependence of aqueous solubility of nitro compounds on temperature and salinity: A COSMO-RS simulation, Chemosphere, 83, 287-294, https://doi.org/10.1016/j.chemosphere.2010.12.065, 2011.

Koch, B. P. and Dittmar, T.: From mass to structure: an aromaticity index for high-resolution mass data of natural organic matter, Rapid Commun. Mass Spectrom., 20, 926-932, https://doi.org/10.1002/rcm.2386, 2006.

Kourtchev, I., Godoi, R. H. M., Connors, S., Levine, J. G., Archibald, A. T., Godoi, A. F. L., Paralovo, S. L., Barbosa, C. G. G., Souza, R. A. F., Manzi, A. O., Seco, R., Sjostedt, S., Park, J. H., Guenther, A., Kim, S., Smith, J., Martin, S. T., and Kalberer, M.: Molecular composition of organic aerosols in central Amazonia: an ultra-high-resolution mass spectrometry study, Atmos. Chem. Phys., 16, 11899-11913, https://doi.org/10.5194/acp-16-11899-2016, 2016.

https://doi.org/10.5194/egusphere-2026-1677
Preprint. Discussion started: 4 May 2026

Krugly, E., Martuzevicius, D., Puida, E., Buinevicius, K., Stasiulaitiene, I., Radziuniene, I., Minikauskas, A., and Kliucininkas, L.: Characterization of gaseous- and particle-phase emissions from the combustion of biomass-residue-derived fuels in a small residential boiler, Energy & Fuels, 28, 5057-5066, https://doi.org/10.1021/ef500420t, 2014.

Křůmal, K., Mikuška, P., and Večeřa, Z.: Polycyclic aromatic hydrocarbons and hopanes in PM_1 aerosols in urban areas, Atmos. Environ., 67, 27-37, https://doi.org/10.1016/j.atmosenv.2012.10.033, 2013.

Laskin, A., Laskin, J., and Nizkorodov, S. A.: Chemistry of atmospheric brown carbon, Chem. Rev., 115, 4335-4382, https://doi.org/10.1021/cr5006167, 2015.

Lee, S. C., Hung, H., Shiu, W. Y., and Mackay, D.: Estimations of vapor pressure and activity coefficients in water and octanol for selected aromatic chemicals at 25°C, Environ. Toxicol. Chem., 19, 2623-2630, https://doi.org/10.1002/etc.5620191102, 2000.

Lelieveld, J., Gromov, S., Pozzer, A., and Taraborrelli, D.: Global tropospheric hydroxyl distribution, budget and reactivity, Atmos. Chem. Phys., 16, 12477-12493, https://doi.org/10.5194/acp-16-12477-2016, 2016.

Li, Y., Fu, T.-M., Yu, J. Z., Zhang, A., Yu, X., Ye, J., Zhu, L., Shen, H., Wang, C., Yang, X., Tao, S., Chen, Q., Li, Y., Li, L., Che, H., and Heald, C. L.: Nitrogen dominates global atmospheric organic aerosol absorption, Science, 387, 989-995, https://doi.org/10.1126/science.adr4473, 2025.

Lin, M., Walker, J., Geron, C., and Khlystov, A.: Organic nitrogen in $PM_{2.5}$ aerosol at a forest site in the Southeast US, Atmos. Chem. Phys., 10, 2145-2157, https://doi.org/10.5194/acp-10-2145-2010, 2010.

Lin, P., Rincon, A. G., Kalberer, M., and Yu, J. Z.: Elemental composition of HULIS in the Pearl River Delta Region, China: results inferred from positive and negative electrospray high resolution mass spectrometric data, Environ. Sci. Technol., 46, 7454-7462, https://doi.org/10.1021/es300285d, 2012a.

Lin, P., Yu, J. Z., Engling, G., and Kalberer, M.: Organosulfates in humic-like substance fraction isolated from aerosols at seven locations in East Asia: a study by ultra-high-resolution mass spectrometry, Environ. Sci. Technol., 46, 13118-13127, https://doi.org/10.1021/es303570v, 2012b.

Lin, P., Fleming, L. T., Nizkorodov, S. A., Laskin, J., and Laskin, A.: Comprehensive molecular characterization of atmospheric brown carbon by high resolution mass spectrometry with electrospray and atmospheric pressure photoionization, Anal. Chem., 90, 12493-12502, https://doi.org/10.1021/acs.analchem.8b02177, 2018.

Ma, Y. J., Xu, Y., Yang, T., Xiao, H. W., and Xiao, H. Y.: Measurement report: characteristics of nitrogen-containing organics in $PM_{2.5}$ in Ürümqi, northwestern China – differential impacts of combustion of fresh and aged biomass materials, Atmos. Chem. Phys., 24, 4331-4346, https://doi.org/10.5194/acp-24-4331-2024, 2024.

Nannoolal, Y., Rarey, J., and Ramjugernath, D.: Estimation of pure component properties: Part 3. Estimation of the vapor pressure of non-electrolyte organic compounds via group contributions and group interactions, Fluid Phase Equilibria, 269, 117-133, https://doi.org/10.1016/j.fluid.2008.04.020, 2008.

Nelson, B. S., Stewart, G. J., Drysdale, W. S., Newland, M. J., Vaughan, A. R., Dunmore, R. E., Edwards, P. M., Lewis, A. C., Hamilton, J. F., Acton, W. J., Hewitt, C. N., Crilley, L. R., Alam, M. S., Şahin, Ü. A., Beddows, D. C. S., Bloss, W. J., Slater, E., Whalley, L. K., Heard, D. E., Cash, J. M., Langford, B., Nemitz, E., Sommariva, R., Cox, S., Shivani, Gadi, R., Gurjar, B. R., Hopkins, J. R., Rickard, A. R., and Lee, J. D.: In situ ozone production is highly sensitive to volatile organic compounds in

https://doi.org/10.5194/egusphere-2026-1677
Preprint. Discussion started: 4 May 2026

Delhi, India, Atmos. Chem. Phys., 21, 13609-13630, https://doi.org/10.5194/acp-21-13609-2021, 2021.

Ng, N. L., Chhabra, P. S., Chan, A. W. H., Surratt, J. D., Kroll, J. H., Kwan, A. J., McCabe, D. C., Wennberg, P. O., Sorooshian, A., Murphy, S. M., Dalleska, N. F., Flagan, R. C., and Seinfeld, J. H.: Effect of NO_x level on secondary organic aerosol (SOA) formation from the photooxidation of terpenes, Atmos. Chem. Phys., 7, 5159-5174, https://doi.org/10.5194/acp-7-5159-2007, 2007.

Nway, N. C., Aung, W. Y., Yi, E. E. P. N., Thant, Z., Yagishita, M., Ishigaki, Y., Suzuki, T., Nakajima, D., Win-Shwe, T.-T., and Mar, O.: Seasonal and regional variation of particulate matter dispersion in Yangon City and Taunggyi City, Myanmar, IOP Conference Series: Earth and Environmental Science, 012003, https://doi.org/10.1088/1755-1315/496/1/012003,

O'Meara, S. P., Xu, S., Topping, D., Alfarra, M. R., Capes, G., Lowe, D., Shao, Y., and McFiggans, G.: PyCHAM (v2.1.1): a python box model for simulating aerosol chambers, Geosci. Model Dev., 14, 675-702, https://doi.org/10.5194/gmd-14-675-2021, 2021.

Pawar, P. V., Mahajan, A. S., and Ghude, S. D.: HONO chemistry and its impact on the atmospheric oxidizing capacity over the Indo-Gangetic Plain, Sci. Total Environ., 947, 174604, https://doi.org/10.1016/j.scitotenv.2024.174604, 2024.

Priestley, M., Le Breton, M., Bannan, T. J., Leather, K. E., Bacak, A., Reyes-Villegas, E., De Vocht, F., Shallcross, B. M. A., Brazier, T., Anwar Khan, M., Allan, J., Shallcross, D. E., Coe, H., and Percival, C. J.: Observations of isocyanate, amide, nitrate, and nitro compounds from an anthropogenic biomass burning event using a ToF-CIMS, J. Geophys. Res-Atmos., 123, 7687-7704, https://doi.org/10.1002/2017JD027316, 2018.

Rickard, A.: Master Chemical Mechanism (MCM) v3.3.1, https://www.mcm.york.ac.uk/MCM, accessed May 2025, 2025.

Rollins, A. W., Browne, E. C., Min, K. E., Pusede, S. E., Wooldridge, P. J., Gentner, D. R., Goldstein, A. H., Liu, S., Day, D. A., Russell, L. M., and Cohen, R. C.: Evidence for NO_x control over nighttime SOA formation, Science, 337, 1210-1212, https://doi.org/10.1126/science.1221520, 2012.

Salvador, C. M. G., Tang, R., Priestley, M., Li, L., Tsiligiannis, E., Le Breton, M., Zhu, W., Zeng, L., Wang, H., Yu, Y., Hu, M., Guo, S., and Hallquist, M.: Ambient nitro-aromatic compounds – biomass burning versus secondary formation in rural China, Atmos. Chem. Phys., 21, 1389-1406, https://doi.org/10.5194/acp-21-1389-2021, 2021.

Samy, S. and Hays, M. D.: Quantitative LC–MS for water-soluble heterocyclic amines in fine aerosols ($PM_{2.5}$) at Duke Forest, USA, Atmos. Environ., 72, 77-80, https://doi.org/10.1016/j.atmosenv.2013.02.032, 2013.

Samy, S., Robinson, J., Rumsey, I. C., Walker, J. T., and Hays, M. D.: Speciation and trends of organic nitrogen in southeastern U.S. fine particulate matter ($PM_{2.5}$), J. Geophys. Res-Atmos., 118, 1996-2006, https://doi.org/10.1029/2012JD017868, 2013.

Saunders, S. M., Jenkin, M. E., Derwent, R. G., and Pilling, M. J.: Protocol for the development of the Master Chemical Mechanism, MCM v3 (Part A): tropospheric degradation of non-aromatic volatile organic compounds, Atmos. Chem. Phys., 3, 161-180, https://doi.org/10.5194/acp-3-161-2003, 2003.

Simoneit, B. R. T., Sheng, G., Chen, X., Fu, J., Zhang, J., and Xu, Y.: Molecular marker study of extractable organic matter in aerosols from urban areas of China, Atmos. Environ. part A.general Topics, 25, 2111-2129, https://doi.org/10.1016/0960-1686(91)90088-O, 1991.

https://doi.org/10.5194/egusphere-2026-1677
Preprint. Discussion started: 4 May 2026

Smith, J. S., Laskin, A., and Laskin, J.: Molecular characterization of biomass burning aerosols using high-resolution mass spectrometry, Anal. Chem., 81, 1512-1521, https://doi.org/10.1021/ac8020664, 2009.

Sun, Y., Luo, H., Li, Y., Zhou, W., Xu, W., Fu, P., and Zhao, D.: Atmospheric organic aerosols: online molecular characterization and environmental impacts, npj Clim. Atmos. Sci., 8, 305, https://doi.org/10.1038/s41612-025-01199-2, 2025.

Tan, Z., Rohrer, F., Lu, K., Ma, X., Bohn, B., Broch, S., Dong, H., Fuchs, H., Gkatzelis, G. I., Hofzumahaus, A., Holland, F., Li, X., Liu, Y., Liu, Y., Novelli, A., Shao, M., Wang, H., Wu, Y., Zeng, L., Hu, M., Kiendler-Scharr, A., Wahner, A., and Zhang, Y.: Wintertime photochemistry in Beijing: observations of RO_x radical concentrations in the North China Plain during the BEST-ONE campaign, Atmos. Chem. Phys., 18, 12391-12411, https://doi.org/10.5194/acp-18-12391-2018, 2018.

Topping, D., Barley, M., Bane, M. K., Higham, N., Aumont, B., Dingle, N., and McFiggans, G.: UManSysProp v1.0: an online and open-source facility for molecular property prediction and atmospheric aerosol calculations, Geosci. Model Dev., 9, 899-914, https://doi.org/10.5194/gmd-9-899-2016, 2016.

Wang, H., Gao, Y., Wang, S., Wu, X., Liu, Y., Li, X., Huang, D., Lou, S., Wu, Z., Guo, S., Jing, S., Li, Y., Huang, C., Tyndall, G. S., Orlando, J. J., and Zhang, X.: Atmospheric processing of nitrophenols and nitrocresols from biomass burning emissions, J. Geophys. Res-Atmos., 125, e2020JD033401, https://doi.org/10.1029/2020JD033401, 2020.

Wang, X. K., Rossignol, S., Ma, Y., Yao, L., Wang, M. Y., Chen, J. M., George, C., and Wang, L.: Molecular characterization of atmospheric particulate organosulfates in three megacities at the middle and lower reaches of the Yangtze River, Atmos. Chem. Phys., 16, 2285-2298, https://doi.org/10.5194/acp-16-2285-2016, 2016.

Xie, Q., Su, S., Chen, J., Dai, Y., and Fu, P.: Increase of nitrooxy organosulfates in firework-related urban aerosols during Chinese New Year's Eve, Atmos. Chem. Phys., 21, 11453-11465, https://doi.org/10.5194/acp-21-11453-2021, 2021.

Xu, W., Sun, Y., Wang, Q., Du, W., Zhao, J., Ge, X., Han, T., Zhang, Y., Zhou, W., Li, J., Fu, P., Wang, Z., and Worsnop, D. R.: Seasonal characterization of organic nitrogen in atmospheric aerosols using high resolution aerosol mass spectrometry in Beijing, China, ACS Earth Space Chem., 1, 673-682, https://doi.org/10.1021/acsearthspacechem.7b00106, 2017.

Xu, Y., Dong, X. N., He, C., Wu, D. S., Xiao, H. W., and Xiao, H. Y.: Mist cannon trucks can exacerbate the formation of water-soluble organic aerosol and $PM_{2.5}$ pollution in the road environment, Atmos. Chem. Phys., 23, 6775-6788, https://doi.org/10.5194/acp-23-6775-2023, 2023.

Yu, K., Zhu, Q., Du, K., and Huang, X. F.: Characterization of nighttime formation of particulate organic nitrates based on high-resolution aerosol mass spectrometry in an urban atmosphere in China, Atmos. Chem. Phys., 19, 5235-5249, https://doi.org/10.5194/acp-19-5235-2019, 2019.

Yu, X., Li, Q., Ge, Y., Li, Y., Liao, K., Huang, X. H., Li, J., and Yu, J. Z.: Simultaneous determination of aerosol inorganic and organic nitrogen by thermal evolution and chemiluminescence detection, Environ. Sci. Technol., 55, 11579-11589, https://doi.org/10.1021/acs.est.1c04876, 2021.

Yu, X., Li, Q., Liao, K., Li, Y., Wang, X., Zhou, Y., Liang, Y., and Yu, J. Z.: New measurements reveal a large contribution of nitrogenous molecules to ambient organic aerosol, npj Clim. Atmos. Sci., 7, 72, https://doi.org/10.1038/s41612-024-00620-6, 2024.

https://doi.org/10.5194/egusphere-2026-1677
Preprint. Discussion started: 4 May 2026

795 Yu, X., Zhou, M., Zhu, S., Qiao, L., Li, J., Ma, Y., Zhang, Z., Liao, K., Wang, H., and Yu, J. Z.: Significant
796 secondary formation of nitrogenous organic aerosols in an urban atmosphere revealed by bihourly
797 measurements of bulk organic nitrogen and comprehensive molecular markers, Atmos. Chem. Phys.,
798 25, 9061-9074, https://doi.org/10.5194/acp-25-9061-2025, 2025.
799 Zeng, Y., Shen, Z., Takahama, S., Zhang, L., Zhang, T., Lei, Y., Zhang, Q., Xu, H., Ning, Y., Huang, Y.,
800 Cao, J., and Rudolf, H.: Molecular absorption and evolution mechanisms of $PM_{2.5}$ brown carbon
801 revealed by electrospray ionization fourier transform–ion cyclotron resonance mass spectrometry
802 during a severe winter pollution episode in Xi'an, China, Geophys. Res. Lett., 47, e2020GL087977,
803 https://doi.org/10.1029/2020GL087977, 2020.
804 Zhang, M., Cai, D., Lin, J., Liu, Z., Li, M., Wang, Y., and Chen, J.: Molecular characterization of
805 atmospheric organic aerosols in typical megacities in China, npj Clim. Atmos. Sci., 7, 230,
806 https://doi.org/10.1038/s41612-024-00784-1, 2024a.
807 Zhang, N., Maung, M. W., Wang, S., Aruffo, E., and Feng, J.: Characterization and health risk assessment
808 of $PM_{2.5}$-bound polycyclic aromatic hydrocarbons in Yangon and Mandalay of Myanmar, Sci. Total
809 Environ., 914, 170034, https://doi.org/10.1016/j.scitotenv.2024.170034, 2024b.
810 Zhang, N., Maung, M. W., Win, M. S., Feng, J., and Yao, X.: Carbonaceous aerosol and inorganic ions
811 of $PM_{2.5}$ in Yangon and Mandalay of Myanmar: seasonal and spatial variations in composition and
812 sources, Atmos. Pollut. Res., 13, 101444, https://doi.org/10.1016/j.apr.2022.101444, 2022.
813 Zhong, Y., Chen, J., Zhao, Q., Zhang, N., Feng, J., and Fu, Q.: Temporal trends of the concentration and
814 sources of secondary organic aerosols in $PM_{2.5}$ in Shanghai during 2012 and 2018, Atmos. Environ.,
815 261, 170034, https://doi.org/10.1016/j.atmosenv.2021.118596, 2021.

816